ELSEVIER

Journal of Photochemistry and Photobiology A: Chemistry 120 (1999) 37–44

Journal of Photochemistry and Photobiology A:Chemistry

Photolysis and thermolysis of azophosphonate model compounds in solid matrices investigated by UV–Visible and infrared spectroscopy

D. Franzke[a,1], J. Kritzenberger[a,2], M. Nobis[b], C. Scherer[b,3], O. Nuyken[b], A. Wokaun[a,c,*]

[a]*Paul Scherrer Institute, CH-5232, Villigen, Switzerland*
[b]*Technical University of Munich, D-85747, Garching, Germany*
[c]*Swiss Federal Institute of Technology (ETHZ)CH-8092, Zürich, Switzerland*

Received 15 June 1998; accepted 7 October 1998

Abstract

Photochemical and thermal decomposition of azophosphonate model compounds **1** and **2** was investigated in solution and in solid KBr matrix by means of UV–Vis and infrared spectroscopy. Photolytically as well as thermolytically induced degradation of both compounds proceeds via nitrogen release; no intermediates could be observed for either thermolytic or photolytic degradation. Determination of an Arrhenius-type activation energy for thermal degradation of **1** reveals that the N=N–P functional group is less stable than other functional groups of the type N=N–X (X=N, S, N(CH_3)N=N). The absence of observable intermediates with a lifetime of seconds or more, in combination with the comparably low activation energy for thermal decomposition, indicates that the thermodynamically stable *trans*-isomer decomposes upon excitation either directly or via highly unstable intermediates. © 1999 Elsevier Science S.A. All rights reserved.

Keywords: Photolysis; Thermolysis; Azophosphonate

1. Introduction

One of the major challenges in polymer chemistry is the design of ‘tailored materials’ which fulfill special requirements for a given application. In recent years, the field of laser induced photoablation has given rise to a high demand for new materials which are suitable for microstructuring by pulsed ultraviolet laser light [1]. The technique utilizes laser pulses of a few nanoseconds length to decompose (polymeric) material into small fragments. This fragmentation induces a subsequent ‘micro-explosion’ as the bulk material is converted into gaseous molecules within the irradiated sample volume, with a concomitant build-up of pressure and expansion. The aim of the process is to remove a predictable amount of substance without affecting the material which is left behind. Compounds to be used in this process are therefore required to decompose rapidly and efficiently when irradiated by UV laser pulses. During photolysis, they should preferentially be degraded into small gaseous fragments which are expelled without polluting the area around the photochemically induced structure.

In recent years, different classes of compounds containing the azo group (–N=N–) have been investigated for this purpose, e.g. triazenes –N=N–NR– [2], pentazadienes –N=N–N(R)–N=N– [3], and hexazadienes –N=N–N(R)–N(R)–N=N– [4]. Those compounds are characterized by high absorption coefficients in the spectral range between 300 and 400 nm. Photochemical excitation of the azo chromophore causes cleavage of the molecule with simultaneous generation of N_2, which may act as a driving gas for the ablation process.

For several representatives, especially for the class of hexazadienes, the azo group is responsible for insufficient storability as the compounds tend to decompose at ambient temperature or even under refrigeration. In order to combine photolability with good storage properties, compounds containing the functional group –N=N–X– (with X = P, S) have been synthesized. This group can be introduced into the backbone as well as into side chains of polymers by several synthetic routes [2,5]. In order to study the photochemical behavior of these structural elements, monomer model compounds were synthesized.

In the present study, we investigate the decay mechanism of two azophosphonate model compounds. Our major attention is focused on the decomposition in solid matrix,

---

[*] Corresponding author. Tel.: +41-56-310-2751; fax: +41-56-310-2199; e-mail: wokaun@psi.ch

[1] Present address: Gretag Imaging AG, CH-8105 Regensdorf, Schweiz

[2] Present address: Patentanwaltskanzlei Diehl, D-80639 München, Germany.

[3] Present address: Bayer AG, D-51368 Leverkusen, Germany

PII: S1010-6030(98)00411-0

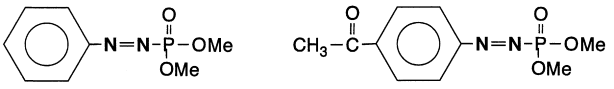

(1) (2)

Scheme 1. Structural formulas of azophosphonate model compounds (**1**) and (**2**) used in present study.

observed by infrared spectroscopy. Potassium bromide was selected as the matrix material, as embedding of the model compounds into organic polymer materials would result in an overlap of the infrared absorption of the matrix with the one of the model compounds.

2. Experimental

2.1. Synthesis of azophosphonate model compounds

For the synthesis of phenylazo-dimethylphosphonate (**1**) (cf. Scheme 1), 10 mmol of aniline hydrochloride was dissolved in 5 ml of diluted hydrochloric acid (20 mmol). 10 ml of water was added, and the solution was cooled to 0°C. 4 ml of a cooled solution of 2.5 M $NaNO_2$ was added dropwise under stirring. The temperature was controlled and kept below 5°C during this step. When the addition of the $NaNO_2$ solution was completed, stirring at 0°C was continued for 30 min. The solution was buffered by the addition of 10 mmol of sodium acetate (0.82 g in 5 ml of H_2O). This was followed by the addition of 10 mmol (1.10 g) dimethylphosphite, and 10 mmol of $NaHCO_3$ (1.68 g dissolved in 20 ml H_2O) was dropped to the reaction vessel. Subsequently, the solution was stirred for 1 h at 0°C, and for another hour at room temperature. The solution showed a deep red color which is typical for azophosphonates. The aqueous solution was extracted with 10 ml $CHCl_2$ three times, and the combined organic phases were extracted 10 times with 10 ml of H_2O to remove inorganic salts and unreacted dimethyl phosphite. The product was dried over $NaSO_4$, filtered, and kept *in vacuo* to remove solvent residuals. The yield was 1.94 g (91% of theory).

The purified product was characterized by means of UV spectroscopy ($\lambda^{\pi\rightarrow\pi^*} = 296$ nm, $\lambda^{n\rightarrow\pi^*} = 489$ nm) and NMR spectroscopy (^{1}H, ^{13}C, ^{31}P).

Synthesis of (acetophenyl) azo-dimethylphophonate (**2**) was carried out in an analogous way by using 4-acetylaniline hydrochloride instead of aniline hydrochloride.

DSC experiments show that the synthesized model compounds are stable with respect to thermal decomposition up to temperatures above 100°C. Nevertheless, for long time conservation, storage in a refrigerator near 0°C is recommended.

2.2. Photolysis in solution

The model compounds were dissolved in organic solvents to achieve an optical density in the range of 1. For monitoring the photochemical reaction by UV spectroscopy, the solutions were transferred into 1 × 1 cm standard quartz cuvettes, and degassed by purging for several minutes with argon immediately before irradiation. UV–Vis measurements were performed using a diode array spectrometer (POLYTEC) equipped with fiber optics (resolution of 2 nm). Typically, five spectra (0.8 s integration time per spectrum) were recorded to obtain a good signal-to-noise ratio. XeCl excimer lasers (Lambda Physik, LPX300 and Compex 205) operating at 308 nm were used as irradiation sources. Pulses of about 20 ns pulse length, with energies between 50 and 500 mJ per pulse, were delivered to the sample. The absorption band at 292 nm was used to monitor the photolytically induced decay, as the band at 490 nm was not detectable with reasonable accuracy at spectroscopically useful concentrations.

2.3. Photolysis in KBr matrix

KBr pellets of about 1 mm thickness were prepared by mixing the model compounds with carefully dried KBr, and densifying the mixture using a standard IR pellet press. The amount of azo compound was adjusted to result in an infrared transmission suitable for recording spectra.

Front and back surfaces of the pellets were irradiated subsequently by UV laser pulses. No significant rise of the temperature due to the irradiation was detectable. After preset numbers of pulses, the irradiation was stopped, and infrared spectra were recorded in a BOMEM DA8002 spectrometer (resolution set to 1 cm^{-1}). Typically, 20 scans were averaged to obtain a good signal-to-noise ratio.

2.4. Thermolysis experiments

For thermolysis experiments, KBr pellets were prepared as described above. The pellets were delivered to a heating chamber which was operated at temperatures between 100 and 140°C. After heating the pellets for a predetermined time, the samples were placed in the BOMEM spectrometer, and infrared spectra were recorded.

Activation energies were determined by monitoring thermal decomposition in a Perkin Elmer FTIR spectrometer. A mixture of (**1**) and KBr was placed into the sample cup of an environmental chamber (Spectra Tech) equipped with temperature control, and investigated in diffuse reflectance geometry. The samples were heated to selected temperatures in an inert gas atmosphere (He), and spectra (4 cm^{-1} resolution) were recorded in intervals of 2 min, to monitor the rate of the decay.

3. Results and discussion

3.1. Photolysis of **1**

A typical photolysis experiment of a solution of **1** in dioxane, monitored by UV–Vis spectroscopy is shown in

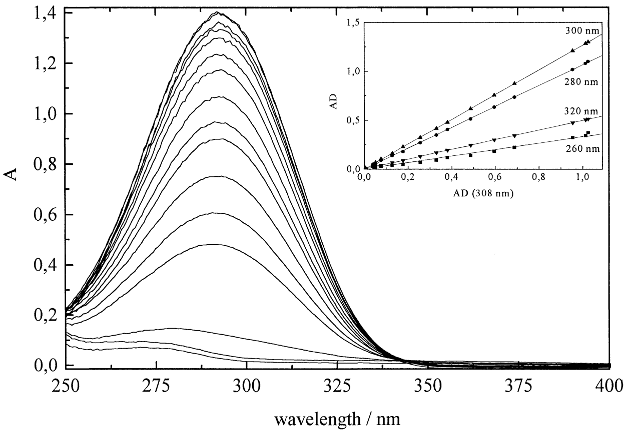

Fig. 1. UV spectra recorded during the photolysis of solution of **1** in dioxane. The solution was irradiated with 308 nm laser pulses (≈80 mJ pulse^{-1}, 20 ns pulse length, 2 Hz repetition rate). The number of pulses delivered to the sample are (from top to bottom) 0, 50, 100, 200, 300, 500, 700, 1000, 1300, 1500, 2000, 2500, 3000, 4000, 5000 (5 Hz), 10000 (10 Hz). Inset: Absorption difference (AD) diagram of the photo reaction. On the abscissa, the values of the absorption difference at the irradiation wavelength of 308 nm are plotted.

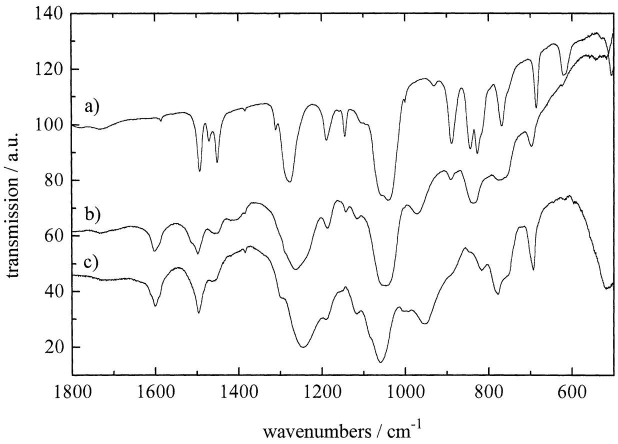

Fig. 2. Photolysis and thermolysis of compound **1**. Infrared spectra of KBr were recorded (a) after preparation, (b) after photolysis with 308 nm pulses, and (c) after thermolysis at 120°C.

Fig. 1. The absorption band exhibiting a maximum at 292 nm decreases, as expected for the decomposition of azo compounds. At the end of the irradiation a band remains with a maximum around 275 nm and a considerably lower absorption coefficient. The spectra were analyzed by absorption difference (AD) diagrams according to the method described by Mauser [6,7]. As can be seen from the inset in Fig. 1, the AD plots are linear, which leads to the conclusion that the mechanism of the reaction is uniform of the type A ⇒ B. This indicates the absence of intermediates with a lifetime in excess of a few seconds. Similar results were obtained when methanol was used as solvent. Furthermore, we varied the conditions for the irradiation, e.g. the pulse energy, and the repetition rate of the laser. In the presence of intermediates having a lifetime between 0.1 and 1 s, one would expect a change in the observed overall decay rate as the laser pulse repetition rate was varied between 1 and 20 Hz; no such dependency was found.

A more extensive investigation of photolytically induced decomposition of azophosphonate polymers, together with the corresponding model compounds, is described at another place [8]. Photolysis experiments in solid matrix are reported next. In Fig. 2, infrared spectra of **1** in KBr matrix in the range of 1800 cm^{-1} to 500 cm^{-1} are shown before (trace a) and after photolysis (trace b). For interpretation, it would have been desirable to reveal infrared spectra in the region between 3100 and 2900 cm^{-1} which is typical for C–H vibrations of aromatic (above 3000 cm^{-1}) and aliphatic (below 3000 cm^{-1}) compounds. Unfortunately, well resolved spectra of the CH-region were detectable only immediately after preparation of the KBr pellets. Due to either irradiation or heating, the signal-to-noise ratio in this region became worse, and a meaningful interpretation of the absorption peaks was not possible. This behavior may be ascribed to increasing scattering of the matrix due to the decomposition of the azo compounds. The scattering is enhanced especially at shorter wavelengths, which leads to higher background intensity.

Comparison of the spectra before (trace a) and after (trace b) irradiation of the sample reveals that in the regime where aromatic C–C vibrations are expected to absorb (around 1600 cm^{-1}), a broad band is growing during photolysis. This behavior indicates that the symmetry of the substitution pattern of the aromatic ring has changed. A support for this assumption is provided by the broadening and the shift of the band at 1493 cm^{-1} towards 1498 cm^{-1}.

The frequencies of the main absorptions involved in the reaction, together with relevant assignments [9,10], are summarized in Table 1. The band at 1471 cm^{-1} (assigned to the N=N bond) disappears, reflecting the expected release of nitrogen during decomposition. Characteristic features of the spectrum of **1** are the band at 1280 cm^{-1} which is assigned to the P=O vibration, and the absorption at 1060 cm^{-1} resulting form the asymmetric stretching vibration of the P–O–C group [9].

The band at 1280 cm^{-1} is broadened after photolysis, which indicated that the molecule fragments in such a way that the P=O bond is affected, with several products giving rise to an inhomogeneous environment. Nevertheless, the P=O bond itself is maintained during the reaction. The band at 1060/1045 cm^{-1} exhibits no shift and only a slight broadening after photolysis.

The band at 1143 cm^{-1} shows decreasing intensity, whereas at 1118 cm^{-1}, a band is growing. The two absorptions at 845 cm^{-1} and 827 cm^{-1}, assigned [9] to the symmetric P–O–C stretching vibration, are replaced by a broad band centered at 835 cm^{-1}. The band at 687 cm^{-1} is shifted towards 698 cm^{-1} while the absorption line at 620 cm^{-1} disappears almost completely. The latter band is assigned [9] to the P–N vibration, and its disappearance is expected since,

Table 1
Main absorption frequencies observed for compound **1** – untreated, after photolysis and after thermolysis

Untreated **1**	Photolysis of **1**	Thermolysis of **1**	Assignment
1587	1603 (+)	1602 (+)	C–C aromatic
1493	1498	1498	C–C aromatic
1471	(−)	(−)	N=N
1452	1453	1458	
1384			
1280	1261	1246	P=O
1189	1189 (−)	1189 (−)	O–CH_3
1143	1143 (−)	(−)	
	1118 (+)	1118 (+)	
1060/1046	1045 (+)	1060 (+)	P–O–C (asym.)
	972 (+)		
		956 (+)	
889	889 (−)	–	
845	835		P–O–C (sym.)
827		819	P–O–C (sym.)
770	770	779	
		753	
687	698	693	
620	–	–	P–N

as mentioned, azophophonates are expected to decompose by the release of nitrogen.

The solvents used in the photolysis experiments using UV–Vis monitoring, as described above, are not suitable for monitoring the decay of the azophosphonates by infrared spectroscopy in view of their strong absorptions overlapping with the bands of the sample. On the other hand, the solvent usually used for recording IR spectra, such as $CHCl_3$ and CCl_4, are not the solvents of choice for investigation of UV photolysis, as they tend to decompose upon UV irradiation with the release of chlorine radicals, which might influence the reaction. Nevertheless, in order to monitor intermediates of the photochemical decay of **1** in solution by infrared spectroscopy, we used a solution of **1** in CCl_4 in a KBr cuvette with 0.1 mm path length in the BOMEM spectrometer and irradiated the sample with an excimer laser. In contrast to the experiments using a KBr matrix, we were able to monitor the region around 3000 cm^{-1} during the photoreaction. Fig. 3 shows that a peak at 2923 cm^{-1} is first growing and then disappears, which is a hint that a stable intermediate is formed during the reaction. In addition, a small peak at 1811 cm^{-1}, already present at the start of the photoreaction, grows and reaches its maximum intensity parallel to the development of the 2923 cm^{-1} peak, and subsequently decreases again. The remaining features of the spectra evolve similarly as observed during the photolytic degradation in a KBr matrix. We note that during the photolysis in solution, an additional peak at 1752 cm^{-1} is created. When the peak at 2923 cm^{-1} reaches its maximum intensity, the peak at 620 cm^{-1}, which is assigned to the P–N bond, is still present (see Fig. 3). This indicates that the intermediate still contains the azo group.

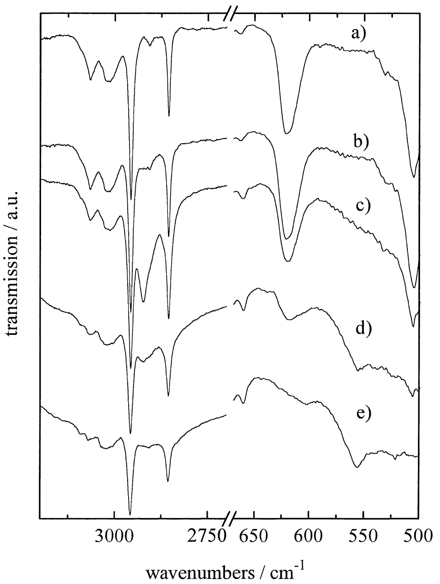

Fig. 3. IR spectra of (**1**) dissolved in CCl_4 after irradiation with (a) 0, (b) 1000, (c)5000, (d)20000, and (e)250000 UV laser pulses at 308 nm.

3.2. *Thermolysis of* **1**

The spectrum obtained at the end if a thermolysis experiment is shown in Fig. 2 (trace c). The overall shape of the spectrum is similar to the one obtained after photolytic decomposition, but exhibits a few distinguishing features. The peak assigned to the P=O vibration (1280 cm^{-1}) is shifted to lower energies (1246 cm^{-1}), whereas the center of the peak assigned to the P–O–C vibration (1060/1046 cm^{-1}) is shifted in the reverse direction while slightly decreasing in intensity. The doublet at 845/827 cm^{-1} of the untreated sample (trace a) is replaced by a peak at 819 cm^{-1} (see also Fig. 5a). This is in contrast to the spectrum recorded after photolytically induced decay where a broad peak at 835 cm^{-1} remained at the end of the reaction. During the thermolytic decomposition, a new peak at 753 cm^{-1} is generated (see also Fig. 5a).

The thermolysis experiments have in common that no intermediate could be detected. This is surprising, especially in comparison to other azo containing compounds such as azo-sulfonates [11], azosulfides [12,13], and pentazadienes [4], which are known to decompose via at least one intermediate which is stable for seconds or minutes.

In order to detect intermediates during thermolysis, we held a KBr sample in an desiccator at room temperature for two days (Fig. 4, trace b) and under vacuum at a temperature of 35°C for three days (Fig. 4, trace c). Comparison with a spectrum of a sample prepared immediately prior to recording the IR-spectrum (trace a) reveals that a sharp band at 1100 cm^{-1} is growing, which is the energy range expected for the P–O–H group (1335–1080 cm^{-1}) [9]. At the same time the doublet at 845 cm^{-1} and 827 cm^{-1} (symmetric P–O–C vibration) is replaced by an absorption at 799 cm^{-1}. The band at

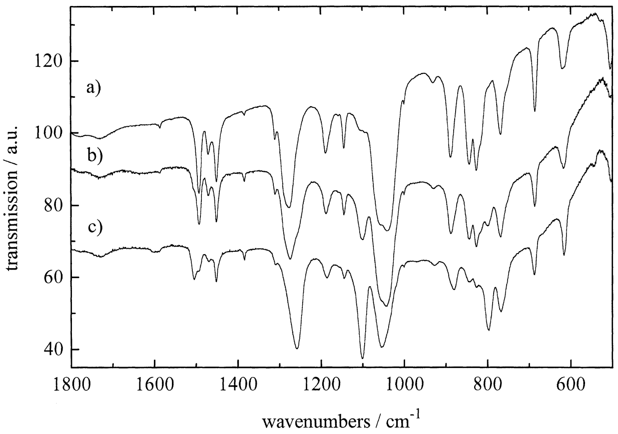

Fig. 4. Infrared spectrum of **1** in KBr (a) freshly prepared, (b) after two days in desiccator at room temperature, and (c) after storage for 3 days at 35°C in vacuo.

1065 cm^{-1}, assigned to the asymmetric P–O–C vibration, decreases and becomes narrower.

A possible interpretation for the above mentioned spectral changes in the replacement of one of the methoxy groups attached to the phosphorus atom by a hydroxy group. This would indicate that hydrolysis takes place, as induced by residual water molecules which may be present in the KBr matrix. We note that the band at 620 cm^{-1}, which we assigned to the P–N bond, is still present after the hydrolysis (trace c). This indicates that the product still contains the N=N functional group, which is released only during thermolytic or photolytic decomposition as described above.

If the hydrolyzed samples are irradiated with an excimer laser, spectra identical to the one obtained after photolysis of a fresh sample (Fig. 2, trace b) are detected. This leads to the conclusion that the hydrolyzed form is not formed during photolytic as well as during thermolytic degradation or, if generated, decomposes very fast in a subsequent step such that it escapes detection.

To quantify the thermal decomposition of **1**, we investigated the decay kinetics according to the method of Arrhenius. For this purpose, we focused on the peak centered at 620 cm^{-1}, which is assigned to the P–N bond. From Fig. 5A it can be seen that this band vanishes almost completely during the thermolysis. For several temperatures, spectra were recorded at preselected times, and the peak area of the P–N band was determined and plotted versus time. Values of the rate constant k were determined by linear regression, and subsequently plotted in a logarithmic scale versus $1/T$. The activation energy E_a was determined as 67 kJ mol^{-1} (Fig. 5B) from linear regression.

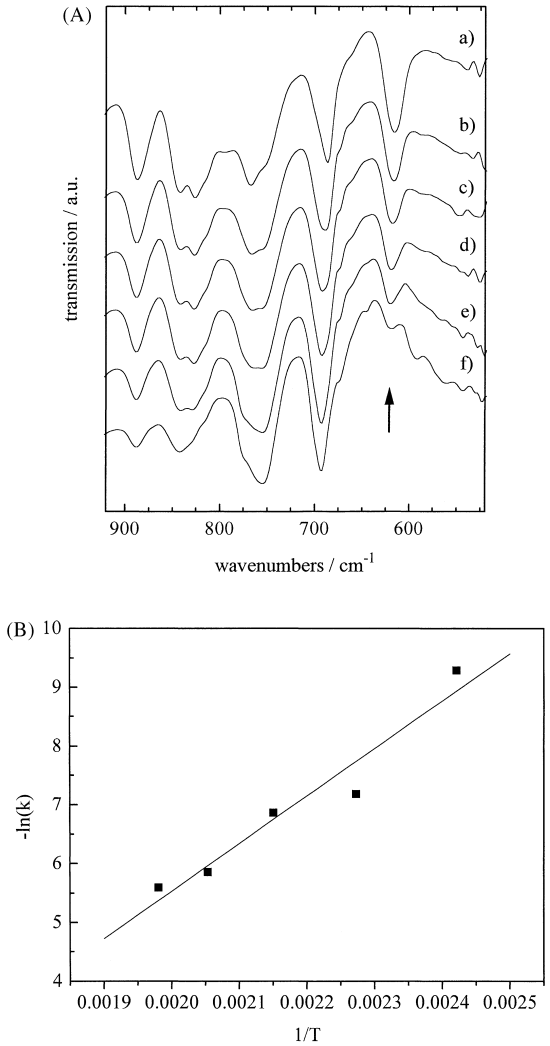

Fig. 5. Thermolysis of compound **1** (A)Spectra were recorded at 200°C after (a) 177s, (b) 318s, (c) 418s, (d) 518s, (e) 819s, and (f) 1922s. The integrated intensity of the peak at 6020 cm^{-1} was used to determined the rate constant k of the reaction. (B) Arrheinus plot for determining the activation energy of the thermolysis reaction. Rate constants were obtained from series of measurements such as those shown in (A), performed at temperatures of 140°C, 192°C, 200°C, 214°C and 232°C, respectively.

Energies of activation of the decomposition of several azo compounds are listed in Table 2. It can be seen that the activation energy for azophosponates is low compared to other azo compounds containing the functional groups N=N–S, N=N–N or N=N–NMe–N=N, respectively.

Table 2
Activation energies (kJ mol^{-1}) for the thermal decomposition of several azo compounds

N=N–S	Pentazadiene polymers	N=N–NMe–N=N	N=N–N	N=N–P
115–143, 152	139	139–154	82–211	67
[12,14]	[3]	[3]	[4]	(This work)

3.3. Photolysis of **2**

To determine the influence of substituents at the benzene ring, we investigated the decay of **2,** where a acetyl group is attached to the ring. Photolysis of **2** in dioxane solution detected by UV–Vis spectroscopy gave rise to results (not shown) that were very similar to those obtained for **1**. There is almost no influence of the substituent at the aromatic ring on the absorption spectrum. The position of the maxima at the beginning and the end of the irradiation pulse sequence are the same as in the case of **1**, but the spectrum of **2** is somewhat broader. Analysis of the spectra using Mauser diagrams provides no hints to the occurrence of stable intermediates.

The infrared spectrum (KBr pellet) of **2** is shown in Fig. 6 before (trace a) and (trace b) photolysis. The main bands involved in the reaction are summarized in Table 3, which includes principal absorption frequencies of acetophenone for comparison. At 2304 cm^{-1}, a new feature arises after photolysis (trace b). This may be interpreted [9] in terms of the formation of a P–H bond via a radicalic side-reaction. This band did not appear during photolysis and thermolysis of **1** in KBr, nor during thermolysis of **2** in KBr.

The band at 1683 cm^{-1} (trace a), which is assigned to the carbonyl vibration, is broadened. This indicates that product compounds are formed having the carbonyl group attached to the aromatic ring but differing in the substitution pattern of the ring.

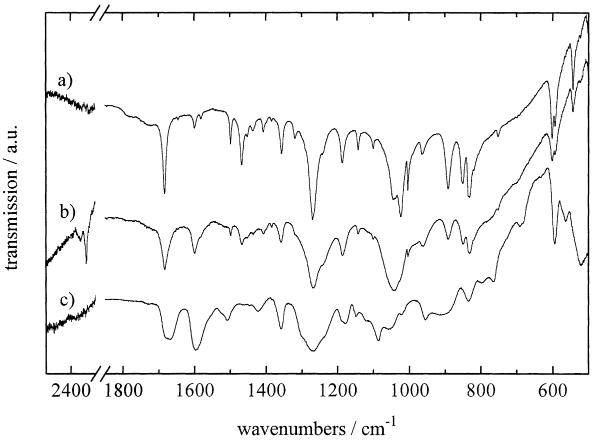

Fig. 6. Photolysis and thermolysis of compound **2**. Infrared spectra in KBr were recorded (a) after preparation, (b) after photolysis with 308 nm pulses, and (c) after thermolysis at 120°C.

The band at 1600 cm^{-1}, which is assigned to an aromatic C–C vibration, shows increasing intensity. The peak at 1469 cm^{-1} (assigned to the N=N vibration) decreases, which indicates the loss of nitrogen. In the region between 1300 cm^{-1} and 800 cm^{-1}, the most significant change in the spectrum is the broadening of the band assigned to the P–O–C group (1043 cm^{-1}). Around 600 cm^{-1}, a doublet is detected exhibiting decreasing intensity during the photolysis. The P–N vibration is expected to absorb in this energy region, hence one peak of the doublet might be due to the latter vibration.

3.4. Thermolysis of **2**

The IR-spectrum of **2** after thermolytic decomposition is shown in trace c of Fig. 6. In contrast to the photolysis, the

Table 3
Main absorption frequencies of **2** untreated, after photolysis and after thermolysis. Spectral data of acetophenone for comparison.

Untreated **2**	Acetophenone[a]	Photolysis of (**2**)	Thermolysis of (**2**)	Assignment
		2304		P–H
1683	1685	1685 (br)	1685 (br)	C=O
1600	1600	1600 (+)	1600 (+)	C–C aromatic
1499		1499	1507	C–C aromatic
1469		1468 (−)		N=N
			1423	
1356	1360	1358	1358	
1267	1267	1267	1270	P=O
1185		1183	1178	O–CH$_3$
1143				
1100				
	1076		1086	
1043		1043	1055	P–O–C (asym.)
1023	1026			
1004	1000	–	–	
962	957	960	957	
892		892 (−)	–	
851		851 (−)	850 (−)	P–O–C (sym.)
833		833 (−)	833 (−)	P–O–C (sym.)
	761		764	
	692		690	
603		603 (−)	–	P–N
595	588	595	595 (+)	

[a] Ref. [10].

formation of the peak at 2304 cm^{-1} (assigned to the P–H vibration) cannot be observed. The peak at 1600 cm^{-1} (aromatic C–C vibration) exhibits a higher intensity compared to the photolysis experiment, and appears rather broad. A reasonable explanation for this behavior is the formation of various products, each containing an aromatic ring with different substituents. The peak of the N=N vibration at 1469 cm^{-1} (trace a) vanishes during thermolysis while a peak at 1423 cm^{-1} appears. The peak at 1267 cm^{-1} becomes very broad, which suggests that different products containing the P=O group are generated. The intense peak at 1043 cm^{-1} (trace a) vanishes, indicating the absence of the P–O–C bond in the product molecules. This behavior may be caused either by a break-off of the methoxy groups, or by further decomposition of the molecule into small fragments. The well-resolved ensemble of the three peaks at 892/851/833 cm^{-1} in the spectrum of **2** (trace a) is reduced to a doublet at 890/833 cm^{-1} with an inverted intensity ratio.

In general, after thermolysis the peaks are broader and the spectrum is less resolved compared to the spectrum after photolysis. A possible interpretation of this behavior is a less selective reaction during thermolysis, and the formation of a larger number of side products. Comparison with the spectrum of acetophenone (cf. Table 3) indicates its presence by the formation of the characteristic peaks at 764 cm^{-1} and 690 cm^{-1}.

After storing a sample of **2** in KBr for several days at room temperature, no change in the spectrum could be observed. This indicates that the acetyl group present in **2** renders a higher stability against hydrolysis to compound **2**, in comparison to **1**.

4. Conclusions

The photolytic and thermolytic decay of the azophosphonate model compounds **1** and **2** has been compared. Irradiation in dioxane solution by excimer laser pulses (308 nm) revealed an identical behavior for both compounds. The maximum at 292 nm decreased, and a new maximum around 275 nm with a lower molar absorption coefficient was formed. Analysis of the spectra according to the method of Mauser [6,7] did not provide any hints for stable intermediates. Variation of the solvent (MeOH) and irradiation conditions, such as pulse energy and pulse repetition frequency, did not influence the photolytic decomposition.

During photolysis in CCl_4, formation of an intermediate was evidenced by IR peaks at 2923 cm^{-1} and 1811 cm^{-1}, which were growing during the first phase of the experiment and subsequently disappeared. However, it has to be kept in mind that in this solvent chlorine radicals may be generated by UV irradiation, which may influence the course of the reaction.

The second technique used for monitoring the decomposition of **1** and **2**, i.e. the recording of infrared spectra of these compounds in KBr matrix, revealed changes in characteristic features, such as the P–O–C and P=O band intensities. During thermolysis as well as photolysis, bands assigned to N=N and P–N vibrations were found to decrease in intensity, indicating the release of nitrogen during decomposition of compounds **1** and **2**. A further common feature of the decomposition reactions of both compounds is the broadening and shift of the band bear 1600 cm^{-1}. This is an indication that the aromatic ring remains undestroyed, with its substitution pattern changed, as expected.

During thermolytic decomposition of **2**, partial formation of acetophenone is observed. Broadening and shift of the band assigned to the P=O vibration for both compounds during photolytic as well as thermolytic decomposition indicate that fragmentation of the azo compounds affects the P=O bond, with several products giving rise to an inhomogeneous environment. This is in agreement with the release of nitrogen during decomposition of azophosphonates **1** and **2**. For both compounds, no intermediates could be detected in the IR spectrum, both during photolysis by UV laser pulses and during thermolysis in an oven. Generally, the bands after thermolysis are broader compared to the bands after photolysis. This leads to the conclusion that the photoreaction is more specific, whereas more side products are generated in the course of themolytic decomposition.

In the case of **2**, a band at 2304 cm^{-1} was created during photolysis, indicating the generation of a P–H bond. A possible explanation for this observation is the replacement of one of the substituents at the phosphorus atom by hydrogen, due to a photochemically induced radical side reaction.

For compound **1**, hydrolysis of the phosphoric acid methyl ester groups, yielding P–OH groups, is occurring during storage of a sample of **1** in KBr for a few days at room temperature. After this hydrolysis reaction, the azo group is still present in the molecule. Compound **2** does not exhibit such a behavior. Even after one week at room temperature, no significant change of the IR spectrum can be observed. This indicates that the carboxy substituent at the phenyl ring stabilizes the molecule against hydrolysis.

Compound **1** exhibits an activation energy of 67 kJ mol^{-1} for the thermal decomposition due to release of N_2. This value is low compared to other compounds containing the –N=N–X– group, such as –N=N–N–, –N=N–S–, and –N=N –NMe–N=N–, respectively, indicating a reduced thermal stability of the –N=N–P– group. Taking into account that no intermediates were detectable for both compounds either during thermolytic or photolytic decomposition, the mentioned comparably low activation energy indicates a direct decomposition of the thermodynamically stable *trans*-isomers of **1** and **2**. Possible intermediates, e.g. *cis*-isomers of the –N=N–P– molecular moiety, are less stable and hence more short-lived (<1 s) than analogous structures of the corresponding –N=N–S– and –N=N–NMe–N=N– compounds [2,12–14].

Acknowledgements

Financial support of this work by a grant of the Swiss National Science Foundation is gratefully acknowledged.

References

[1] O. Nuyken, C. Scherer, A. Baindl, A. Brennen, U. Dahn, R. Gärtner, S. Kaiser-Röhrich, R. Kollefrath, P. Matusche, B. Voit, Progr. Polym. Sci. 22 (1997) 93.

[2] J. Stebani, Ph.D. thesis, University of Bayreuth, 1993.

[3] A. Baindl, Ph.D. thesis, Technical University of Munich, 1996.

[4] Th. Lippert, A. Wokaun, J. Stebani, O. Nuyken, J. Ihlemann, Angew. Makormol. Chem. 213 (1993) 127.

[5] U. Dahn, Ph.D. thesis, Technical University of Munich, 1997.

[6] H. Mauser, Z. Naturforsch. 23b (1968) 1021.

[7] H. Mauser, H.J. Niemann, R. Krestchmer, Z. Naturforsch. 27b (1972) 1349.

[8] Th. Kunz, Ch. Hahn, A. Wokaun, Adv. Mater. 10 (1998) 786.

[9] G. Socrates, Infrared Characteristic Group Frequencies, Wiley, New York, 1994.

[10] B. Schrader, Raman/Infrared Atlas or Organic Compounds, VCH, Weinheim, 1989.

[11] D. Franzke, B. Voit, O. Nuyken, A. Wokaun, Mol. Phys. 77 (1992) 397.

[12] J. Kristzenberger, D. Franzke, Th. Kunz, A. Lang, O. Nuyken, A. Wokaun, Angew. Makromol. Chem. 254 (1998) 17.

[13] D. Franzke, J. Kritzenberger, E. Ortelli, A. Baindll, O. Nuyken, A. Wokaun, J. Photochem. Photobiol. A 112 (1998) 63.

[14] O. Nuyken, A. Lang, Angew. Makromol. Chem. 129 (1995) 230.